Photocatalytic degradation of metoprolol tartrate in suspensions of two TiO2-based photocatalysts with different surface area. Identification of intermediates and proposal of degradation pathways.

Photocatalytic degradation of metoprolol tartrate in suspensions of two TiO_2-based photocatalysts with different surface area. Identification of intermediates and proposal of degradation pathways

Biljana Abramović[1*], Sanja Kler[1], Daniela Šojić[1], Mila Laušević[2], Tanja Radović[2], Davide Vione[3]

[1] *Department of Chemistry, Biochemistry and Environmental Protection, Faculty of Sciences, University of Novi Sad, Trg D. Obradovića 3, 21000 Novi Sad, Serbia*

[2] *Faculty of Technology and Metallurgy, University of Belgrade, Karnegijeva 4, 11120 Belgrade, Serbia*

[3] *Dipartimento di Chimica Analitica, Università di Torino, Via Pietro Giuria 5, 10125 Torino, Italy*

*Professor Biljana Abramović
Department of Chemistry, Biochemistry and Environmental Protection
Faculty of Sciences
Phone: +381 21 4852753
Fax: +381 21 454065
e-mail: biljana.abramovic@dh.uns.ac.rs
Trg D. Obradovića 3
21000 Novi Sad
Serbia

E-mail address: sanja.kler@dh.uns.ac.rs (Sanja Kler)
daniela.sojic@dh.uns.ac.rs (Daniela Šojić)
milal@tmf.bg.ac.rs (Mila Laušević)
tradovic@tmf.bg.ac.rs (Tanja Radović)
davide.vione@unito.it (Davide Vione)

Abstract

This study investigated the efficiency of the photocatalytic degradation of metoprolol tartrate (MET), a widely used β_1-blocker, in TiO_2 suspensions of Wackherr's "Oxyde de titane standard" and Degussa P25. The study encompassed transformation kinetics and efficiency, identification of intermediates and reaction pathways. In the investigated range of initial concentrations (0.01–0.1 mM), the photocatalytic degradation of MET in the first stage of the reaction followed approximately a pseudo-first order kinetics. The TiO_2 Wackherr induced a significantly faster MET degradation compared to TiO_2 Degussa P25 when relatively high substrate concentrations were used. By examining the effect of ethanol as a scavenger of hydroxyl radicals ($^{\bullet}OH$), it was shown that the reaction with $^{\bullet}OH$ played the main role in the photocatalytic degradation of MET. After 240 min of irradiation, the reaction intermediates were almost completely mineralized to CO_2 and H_2O while the nitrogen was predominantly present as NH_4^+. Reaction intermediates were studied in detail and a number of them were identified using LC–MS/MS (ESI+), which allowed the proposal of a tentative pathway for the photocatalytic transformation of MET as a function of the TiO_2 specimen.

Keywords: Metoprolol tartrate; β_1-blocker; Photocatalytic degradation; Titanium dioxide; Photocatalytic transformation pathways

Highlights

►Kinetics and efficiency of photocatalytic degradation of the β_1-blocker metoprolol tartrate (MET). ►Two TiO_2 specimens employed. ►Faster degradation of MET, but slower mineralization, obtained with the TiO_2 specimen having lower surface area. ►Photocatalytic transformation pathways of MET including mineralization.

1. Introduction

When speaking of pollutants in the environment one usually thinks of chemicals that are used to treat plants and soil, of radioactive wastes and of exhaust gases. Active components of drugs have slowly – one might say, 'by the back door', entered the environment, with the primary purpose of helping people. The notion of active pharmaceutical ingredients (APIs) includes highly bioactive compounds that are used in the treatment or prevention of diseases, thanks to their reaction with specific targets in the animal or human body such as receptors or enzymes. Due to their increasing consumption, growing emissions of APIs affect the natural environment from hospitals, pharmaceutical industries or domestic waters. In the latter case, incorrect disposal of non-used or expired drugs and human excretions after partial metabolism of the drugs by the body are the main pathways involved [1]. The use of antibiotics in cattle breeding is a further, important route of pharmaceuticals to the environment [2].

Although APIs are present in water at low levels, their continuous inflow may constitute a risk for water and land organisms, either as an acute threat or through bioaccumulation. APIs have been detected in ground and surface water [3–5], drinking water [6,7], ocean water, sediment and soil [8]. In the latest years there has been a tendency to synthesize drugs that are resistant to common biotransformation processes, with the purpose of protracting their persistence in the organism. However, very stable molecules are obtained as a result [9,10], the environmental occurrence of which at either low or high concentrations can bring harmful toxicological effects [11,12]. The persistence of APIs is not the only problem, there is also the possibility that the excreted conjugates between the drug and glucuronic acid are converted back to the parent compound, which could give a multiplied detrimental effect [1].

The metoprolol tartrate salt {MET, *1-[4-(2 methoxy ethyl)phenoxy]-3-(propan-2-yl amino)propan-2-ol tartrate (2 : 1), CAS No 56392-17-7,* $(C_{15}H_{25}NO_3)_2\ C_4H_6O_6$, $M_r = 684.81$} is a selective β-blocker that is used to treat a variety of cardiovascular diseases, such as hypertension, coronary artery disease and arrhythmias. It blocks the action of epinephrine and norepinephrine on the β-adrenergic receptors in the body, primarily in the heart [13]. MET is characterized by an increasing use in recent years and, as a consequence, its occurrence in aqueous effluents is expected to increase as well [14,15]. MET shows slow direct phototransformation and/or hydrolysis [16,17]. An efficient way to deal with this problem is the degradation of the drug by advanced oxidation processes (AOPs) based on the formation

of hydroxy ($^{\bullet}$OH) and other radicals. Such reactive transients oxidize toxic and non-biodegradable compounds to yield different intermediates and to produce inert final products after a sufficient reaction time [18]. MET contains a secondary amine group and a weakly/moderately activated aromatic ring that are likely targets of molecular ozone and of $^{\bullet}$OH [13]. Yang et al. investigated the degradation of selected β-blockers (atenolol, metoprolol and propranolol) in aqueous suspensions of TiO_2 Degussa P25 and proposed a preliminary mechanism of degradation of these compounds [19]. Romero et al. have also investigated and compared the degradation intermediates of metoprolol and propranolol by AOPs [20].

The aim of this work was to make a detailed comparison of the kinetics and mechanism of photodegradation of MET, sensitized by TiO_2 Wackherr and Degussa P25 in aqueous solution under a variety of experimental conditions. The effects of the initial concentration of MET and of catalyst loading were studied, along with the presence of $^{\bullet}$OH scavengers. An attempt has also been made to identify the intermediates formed during the photooxidation process and to propose possible reaction pathways for the photocatalytic degradation of MET in UV-irradiated aqueous suspensions of TiO_2.

2. Materials and methods

2.1. Chemicals and solutions

All chemicals were of reagent grade and were used without further purification. The drug (±)-Metoprolol(+)-tartrate salt (Sigma–Aldrich) was used as received (≥99% purity); 85% H_3PO_4 was purchased from Lachema, Neratovice; 96% ethanol was obtained from Centrohem, Stara Pazova; 99.8% acetonitrile (ACN) was a product of J.T. Baker. All solutions were made using doubly distilled water. The TiO_2 Degussa P25 (75% anatase and 25% rutile, surface area 50 ± 1.0 m^2 g^{-1}, crystallite size about 20 nm, non-porous) and Wackherr's "Oxyde de titane standard" (100% anatase, surface area 8.5±1.0 m^2 g^{-1}, crystallite size 300 nm, hereafter "TiO_2 Wackherr"), produced by the sulfate process were used as photocatalysts [21].

2.2. Photodegradation procedures

Photocatalytic degradation was carried out in a cell made of Pyrex glass (total volume of *ca.* 40 mL, liquid layer thickness 35 mm), with a plain window on which the light beam was focused. The cell was equipped with a magnetic stirring bar and a water circulating jacket. A 125 W high-pressure mercury lamp (Philips, HPL-N, emission bands in the UV region at 304,

314, 335 and 366 nm, with maximum emission at 366 nm) together with an appropriate concave mirror was used as the radiation source. The output of the mercury lamp was calculated to be *ca.* 8.8×10^{-9} Einstein mL^{-1} min^{-1} (potassium ferrioxalate actinometry).

In a typical experiment, and unless otherwise stated, the initial MET concentration was 0.05 mM and the TiO_2 loading (Degussa P25 or Wackherr) was 1.0 mg mL^{-1}. The total suspension volume was 20 mL. The aqueous suspension of TiO_2 was sonicated (50 Hz) in the dark for 15 min before illumination, to uniformly disperse the photocatalyst particles and attain adsorption equilibrium. Before irradiation, the suspension thus obtained was thermostated at 25±0.5 ºC in a stream of O_2 (3.0 mL min^{-1}). During irradiation, the mixture was stirred at a constant rate under continuous O_2 flow. Control experiments were also carried out under O_2 flow but by stopping the irradiation. These tests showed that the O_2 flow did not cause losses of volatile compounds during the degradation. All experiments were performed at the natural pH (*ca.* 7). Where applicable, ethanol (400 μL) was added as $^{\bullet}OH$ scavenger.

2.3. Analytical procedures

For the LC–DAD kinetic studies of MET photodegradation, aliquots of 0.50 mL were taken from the reaction mixture at the beginning of the experiment and at regular time intervals. Aliquot sampling caused a maximum volume variation of *ca.* 10% in the reaction mixture. The suspensions were filtered through Millipore (Millex-GV, 0.22 μm) membrane filters to eliminate the photocatalyst. Lack of adsorption of MET on the filters was preliminarily checked. After that, a 20-μL sample was injected and analyzed on an Agilent Technologies 1100 Series liquid chromatograph, equipped with an Eclypse XDB-C18 column (150 mm × 4.6 mm i.d., particle size 5 μm, 25 °C). The UV/vis DAD detector was set at 225 nm (wavelength of MET maximum absorption), as well as at 210, 260, 270 and 280 nm for the monitoring of the intermediates. The mobile phase (flow rate 0.8 mL min^{-1}) was a mixture of ACN and water, the latter acidified with 0.1% H_3PO_4, with the following gradient: 0 min 15% ACN which increased to 30% ACN in 5 min, after which 30% ACN was constant for 5 min; post time was 3 min. Reproducibility of repeated runs was around 3–10%.

Absorption spectra were recorded on a double-beam T80+ UV–vis spectrophotometer (UK) at a fixed slit width (2 nm), using 1 cm quartz cells and computer-loaded UV Win 5 data software. Kinetics of the aromatic ring degradation was monitored at 225 nm [22].

For ion chromatographic determinations, aliquots of 3 mL of the reaction mixture were taken at regular time intervals, filtered through membrane filters and analyzed on an ion

chromatograph Dionex ICS 3000 Reagent Free IC system with conductometric detector. For anions determination, use was made of an IonPac AS18 column (250 mm × 4 mm i.d., bead diameter 8 μm). The mobile phase was KOH solution (20–40 mM) at a flow rate of 1 mL min^{-1}. Cations were determined using an IonPac CS12A column (250 mm × 4 mm i.d., bead diameter 7.5 μm) and the mobile phase was a 40 mM solution of methanesulfonic acid at 1 mL min^{-1} flow rate.

Changes in the pH during the degradation were monitored using a combined glass electrode (pH-Electrode SenTix 20, WTW) connected to a pH-meter (pH/Cond 340i, WTW). In all cases, correlation coefficients obtained for the calibration curves were higher than 0.98.

For the LC–MS/MS (ESI+) evaluation of intermediates, a more concentrated solution (3 mM) of MET was prepared. Aliquots were taken at the beginning of the experiment and at regular time intervals during the irradiation. It followed filtration to separate the TiO_2 particles. A Surveyor LC system (Thermo Fisher Scientific) was used for the separation of the analytes on an Agilent Technologies reverse-phase Zorbax Eclipse® XDB-C18 column (75 mm × 4.6 mm i.d., particle size 3.5 μm, 20 °C). An Agilent Technologies guard column (12.5 mm × 4.6 mm i.d., particle size 5 μm) was used. The mobile phase consisted of methanol (A) and 10% acetic acid (B), with the following gradient: 0 min – A 30%, B 70%; 15 min – A 60%, B 40%; 15.10 min – A 100%, B 0%; 19 min – A 100%, B 0%; 19.10 min – A 30%, B 70%. The initial conditions were re-established and held for 15 min. The flow rate of the mobile phase was 0.6 mL min^{-1}, the injection volume was 10 μL. An LCQ Advantage quadrupole ion trap mass spectrometer (Thermo Fisher Scientific) equipped with an electrospray ionization unit was used to perform the mass spectrometric analysis. Spray voltage was set to 4.5 kV and sheath gas flow rate optimized at 23 au (arbitrary units, from a scale of arbitrary units in the 0–100 range defined by the LCQ Advantage system). Positive electrospray (capillary voltage of 4.0 kV) was used for the ionization of the analytes, with nitrogen (temperature 290 ^{0}C, flow 11 L min^{-1}) as the nebulizer gas. High-purity nitrogen was used as the collision gas. Full scan mode (*m*/*z* range 70–500, scan time 200 ms, cone voltage 80 V) was used to select the precursor ion for MET and each intermediate, as well as to examine isotopic peaks distribution (Table 1). Then, product ion scan MS/MS mode (cone voltage 60 V, scan time 200 ms, collision energy 28–35%, 100% rel. abundance set for precursor ions) was used for structure elucidation of each degradation intermediate. Finally, the multiple reaction monitoring (MRM) mode (parameters are given in Table 1) was used for obtaining peak areas of the analytes, in order to track the reaction kinetics.

(Table 1)

For total organic carbon (TOC) analysis, aliquots of 10 mL of the reaction mixture were taken at regular time intervals, diluted to 25 mL and analyzed after filtration on an Elementar Liqui TOC II analyzer according to Standard US 120 EPA Method 9060A.

3. Results and discussion

3.1. Effect of the kind of TiO_2

The photocatalytic activity of TiO_2 Wackherr was compared to that of the most often used TiO_2 Degussa P25 under UV irradiation (Fig. 1). As can be seen from the figure, significant MET degradation could be observed under UV and the process involving TiO_2 Wackherr was significantly faster compared to the direct photolysis and to the transformation in the presence of Degussa P25. Also, it can be noticed that the variety and amount of intermediates depended on the type of catalyst (Fig. 2). The faster degradation of MET in the presence of TiO_2 Wackherr compared to Degussa P25 is an interesting result, although it is hardly unexpected [21,23,24]. Note that TiO_2 Wackherr has much larger particles than Degussa P25 (3–4 times larger average radii in solution), which produces a surface area that is almost six times lower [21].

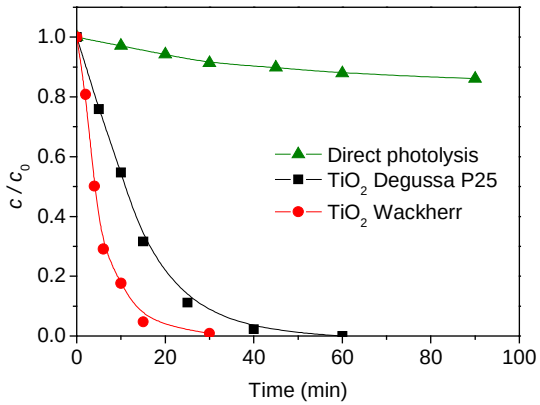

Fig. 1. Kinetics of the photolytic and photocatalytic degradation of MET (initial concentration c_0 = 0.05 mM). When present, the TiO_2 loading was 1.0 mg mL^{-1}.

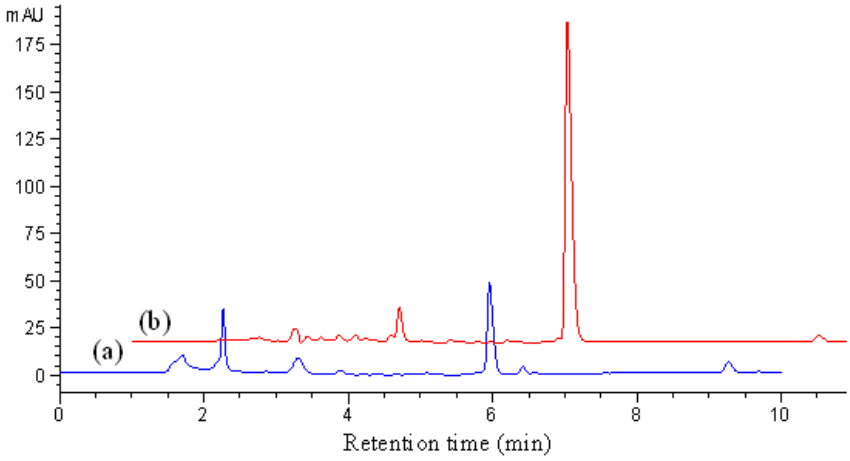

Fig. 2. Chromatograms obtained after 10 min of MET (c_0 = 0.05 mM) degradation under UV irradiation in the presence of TiO_2 Wackherr (a) and Degussa P25 (b). λ_{det} = 225 nm, t_R(MET) = 5.8 min.

Fig. 1 also shows that MET can be degraded by direct photolysis upon irradiation in the near-UV region, in the absence of TiO_2. However, the direct photolysis is significantly slower than the photocatalytic processes. It should also be considered that radiation absorption and scattering by TiO_2 can substantially inhibit direct photolysis under photocatalytic conditions [25]. In the presence of a TiO_2 loading of 1.0 mg mL^{-1}, UV radiation absorption by diluted species in solution can safely be neglected [21,24]. Therefore, the rate of MET direct photolysis is expected to be negligible under the adopted photocatalytic conditions.

All time evolution curves at the beginning of the reaction could be fitted reasonably well by an exponential decay function according to a pseudo-first order kinetic model. The apparent first-order rate constant, obtained by data fit with the equation that follows, was used in all subsequent plots to calculate the rate of MET degradation:

$$-\frac{dc}{dt} = k_a c_0$$

In the equation, c is the MET concentration at the time t, c_0 its initial concentration and k_a the apparent first-order rate constant. The fit of the experimental data ($\ln c = \ln c_0 + k_a t$) enabled the calculation of the pseudo-first order rate constant k_a (the linear correlation coefficients were in the range of 0.983–0.999). The initial rates (R) of MET transformation were calculated as the product $k_a c_0$.

The kinetic curves shown in Fig. 1 were the basis to calculate the initial rate of MET degradation. It was found that in the presence of TiO_2 Wackherr, R was approximately 2.5 times higher than with Degussa P25 {R(Wackherr) = 9.2 µM min^{-1}, irradiation time up to 10

min, *vs.* *R*(Degussa P25) = 3.8 µM min^{-1}, irradiation time up to 20 min}. The direct photolysis rate (*R* = 0.1 µM min^{-1}, irradiation time up to 20 min) was lower by about two orders of magnitude compared to *R*(Wackherr).

MET is remarkably stable in aqueous solution: no modification was observed in a MET solution kept in the dark for 550 days, which allows excluding *e.g.* hydrolysis as a significant transformation pathway.

3.2. Effect of the initial concentration of MET

The effect of the initial concentration of MET on the rate of its photodegradation was investigated in the range of concentrations from 0.01 to 0.1 mM (Fig. 3)**.** The rate of photocatalytic degradation increased with increasing MET from 0.01 to 0.08 mM. In the case of TiO_2 Wackherr the rate appears to reach a plateau above 0.08 mM MET, while in the presence of TiO_2 Degussa P25 the rate was maximum for 0.08 mM MET.

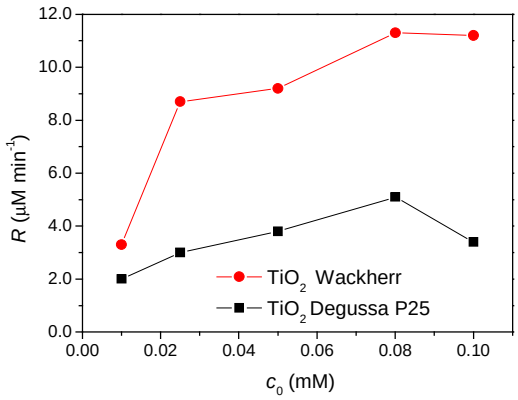

Fig. 3. Effect of the initial MET concentration (c_0) on the initial rate of its decomposition (*R*), in the presence of TiO_2 Wackherr and of Degussa P25. In both cases the TiO_2 loading was 1.0 mg mL^{-1}. The degradation rate *R* was determined for the first 10 and 20 min of irradiation in the case of TiO_2 Wackherr and of Degussa P25, respectively.

A saturative trend of the rate with increasing MET concentration would be accounted for by the scavenging of reactive species by the substrate. The reaction of MET with $^{\bullet}OH$ and h^+ on the surface of TiO_2 is in competition with the thermal recombination processes $^{\bullet}OH/e^-$ and h^+/e^-. An excess of the substrate would completely inhibit the recombination reactions, so that the rate of substrate degradation could at most be equal to the trapping rate of $^{\bullet}OH$ and h^+ on the surface of TiO_2 [26–28]. However, this explanation would not account for the trend with a

maximum of R vs. c_0 that was observed in the case of Degussa P25. The decrease of R with c_0 after the maximum is usually accounted for by the recombination reactions between partially oxidized transients, derived from the substrate, and the conduction-band electrons [29]. Indeed, organic compounds usually require the loss of pairs of electrons to yield stable oxidation intermediates. Abstraction of one electron from the substrate would yield a radical transient, which could either undergo further oxidation to a non-radical intermediate, or react with an electron to give back the initial substrate. The second process, so-called back or recombination reaction, is favored by an elevated substrate concentration and accounts for the decrease of the initial transformation rates with increasing substrate [23,29].

The trends reported in Fig. 3 suggest that the back reactions are more important in the case of Degussa P25 compared to Wackherr. Note that MET degradation rates do not differ much among the two photocatalysts for 0.01 mM substrate, while the difference becomes considerably more important at higher MET concentration. This means that most of the transformation rate difference between Wackherr and Degussa P25 at, say, 0.05 mM MET or higher would be accounted for by the back reactions. Similar results have been observed in the case of benzoic acid and of picloram [21,24].

3.3. Effect of catalyst loading

The effect of the loading of TiO_2 Wackherr and of Degussa P25 on the efficiency of MET photodegradation was examined in the loading range from 0.5 to 5.0 mg mL^{-1} (Fig. 4). As can be seen in Fig. 4, the effect of catalyst loading on the degradation rate was similar in both cases. Indeed, with an increase of the TiO_2 loading up to 1 mg mL^{-1} the degradation rate increased to decrease afterwards, but the rate of MET removal was significantly higher with TiO_2 Wackherr. The most likely reason for the difference between the two photocatalysts is that, at 0.05 mM MET, the back reactions affect Degussa P25 more than TiO_2 Wackherr.

One might think that an increase of the catalyst loading above an optimum value has no effect on the photodegradation rate, because all the light available is already utilized. However, a higher TiO_2 loading leads to the aggregation of the photocatalyst particles that decreases the contact surface area between reactant and photocatalyst. The consequence is a decrease of the number of active sites and a lower rate of photodegradation. Besides, the increase of the solution turbidity and of light dispersion by the particles may also produce a lower degradation rate [21,30,31].

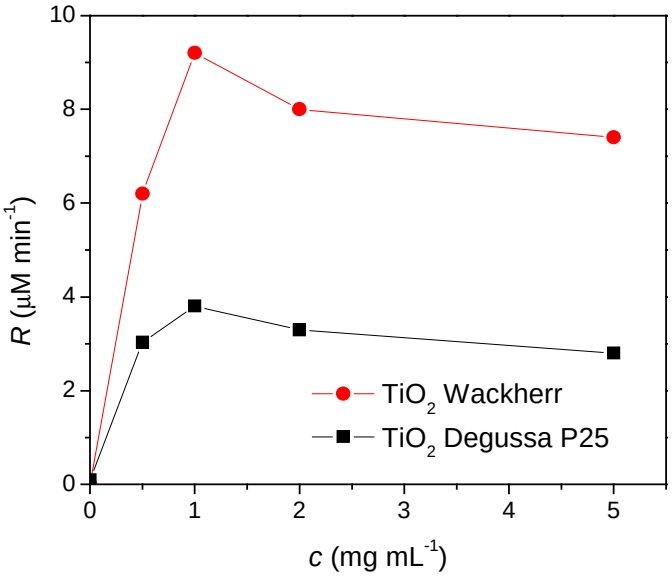

Fig. 4. Influence of TiO_2 loading on MET (c_0 = 0.05 mM) degradation rate determined for the first 10 min irradiation (in the case of TiO_2 Wackherr) and 20 min irradiation (in the case of TiO_2 Degussa P25).

3.4. Effect of ethanol as hydroxyl radical scavenger

To check whether the photocatalytic degradation of MET takes place via $^{\bullet}OH$, ethanol (400 μL, *i.e.* 0.34 M in the final solution) was added to the reaction mixture containing MET and TiO_2 Wackherr or Degussa P25.

The results presented in Fig. 5 show a considerable inhibition by ethanol of the photocatalytic degradation of MET. With Degussa P25, the reaction was about three times slower with 0.34 M ethanol (R = 1.2 μM min^{-1}) than in the absence of the alcohol (R = 3.8 μM min^{-1}). In the case of TiO_2 Wackherr the difference was more marked: the rate with ethanol (R = 1.4 μM min^{-1}) was seven times lower than without ethanol (R = 9.2 μM min^{-1}).

Photocatalytic degradation processes can involve either reaction between the substrate and surface-adsorbed $^{\bullet}OH$ groups, or direct charge-transfer processes with valence-band holes [21]. Aromatic compounds are usually reactive with both $^{\bullet}OH$ and the holes, while addition of alcohols or glycols is a good strategy to selectively block the $^{\bullet}OH$-mediated processes. Indeed, alcohols are usually poorly reactive toward the holes [32,33].

The experimental data suggest that the photocatalytic degradation of MET mainly proceeds via $^{\bullet}OH$, especially in the case of TiO_2 Wackherr, while valence-band holes are

expected to play a secondary role. The more marked ethanol effect on TiO_2 Wackherr compared to Degussa P25 suggests that holes might play a somewhat more important role in the presence of the latter photocatalyst. The fact that reactivity with holes is more important in the case of Degussa P25 than for TiO_2 Wackherr has already been observed with picloram [24].

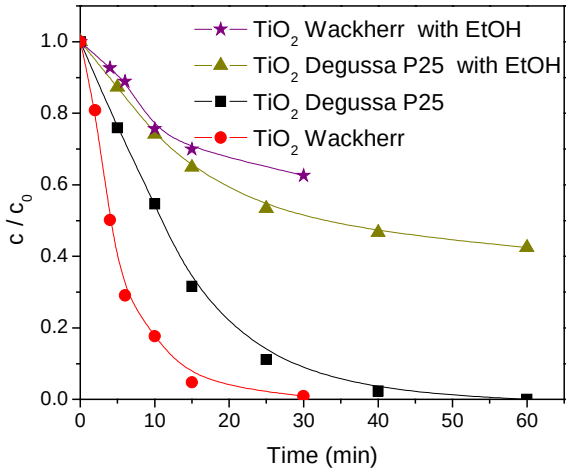

Fig. 5. Effect of 0.34 M ethanol on the efficiency of degradation of MET (c_0 = 0.05 mM) in the presence of TiO_2 (1 mg mL^{-1}).

In the case of MET, however, the importance of the holes in the degradation over both photocatalysts is expected to be higher than for picloram, for which the addition of ethanol caused a definitely more marked inhibition of the degradation [24]. Usually, reaction with holes is more important for hydrophobic compounds that are repelled from the aqueous solution and are thus more likely to undergo adsorption over the photocatalyst surface [33a]. The longer lateral chain of MET compared to picloram could possibly account for a higher degree of surface adsorption and hole reaction.

3.5. Evaluation of the degree of mineralization

MET contains a secondary amino group, thus it could be expected that NH_4^+ and/or NO_2^- / NO_3^- ions might be formed in the photocatalytic degradation [34]. Both ammonium and nitrate were monitored, and it appeared that the ammonium concentration was much higher (Fig. 6a/b, curves #5, compared to curves #4 for nitrate). After irradiation for 120 min, 63% of nitrogen was transformed in the presence of Degussa P25 and only 23% in the presence of

TiO_2 Wackherr. The respective shares of ammonium were 53% and 20% of the total initial nitrogen.

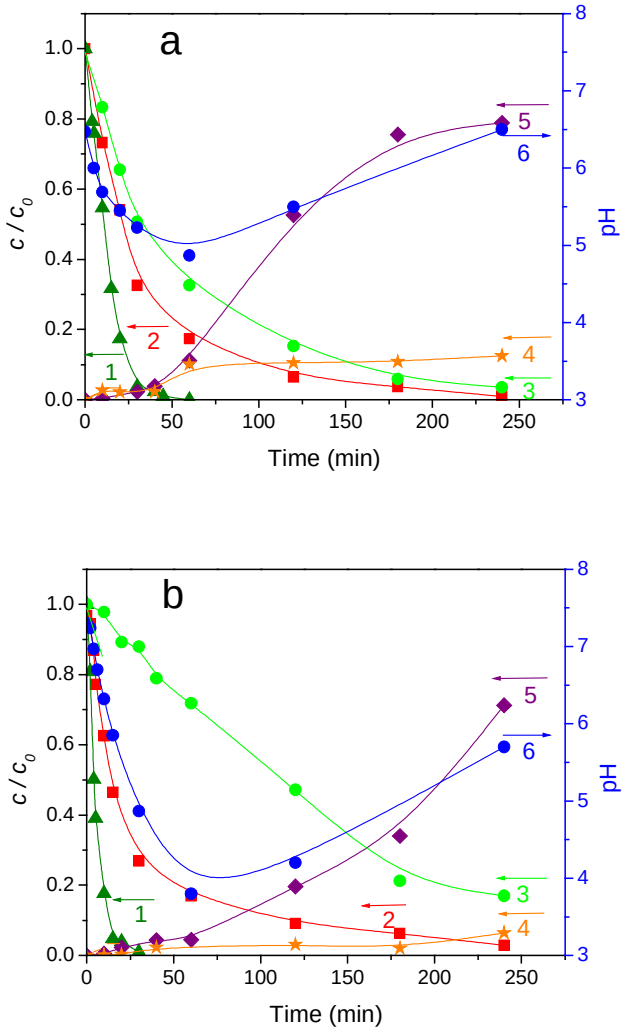

Fig. 6. Photocatalytic degradation of MET (c_0 = 0.05 mM) in the presence of TiO_2 Degussa P25 (a) and TiO_2 Wackherr (b). (1) disappearance of MET (LC–DAD, λ = 225 nm); (2) disappearance of the aromatic ring (spectrophotometry, λ = 225 nm); (3) TOC trend; (4) evolution of NO_3^-; (5) evolution of NH_4^+; (6) pH.

Figure 6a/b also shows the kinetic curves for aromatic ring degradation (curves #2, 225 nm absorption). The degradation of the aromatic ring in the presence of Degussa P25 is about 2.5 times slower compared to the MET disappearance. In the presence of TiO_2 Wackherr, the aromatic ring degradation is even four times slower compared to MET disappearance. These findings indicate the presence of different intermediates with an aromatic ring. The large difference in MET degradation rates between TiO_2 Wackherr and Degussa P25 ensures that

aromatic ring disappearance is still faster with TiO_2 Wackherr (2.1 μM min^{-1}) than for Degussa P25 (1.5 μM min^{-1}). However, the MET/aromatic ring degradation rate ratios (2.5 for Degussa P25 *vs.* 4 for Wackherr) suggests that TiO_2 Wackherr induces formation of a higher amount of intermediates with aromatic ring compared to Degussa P25. This is in agreement with the chromatograms reported in Fig. 2a/b.

Monitoring of the kinetics of photocatalytic degradation via the change in pH has mainly been carried out for simple molecules, where practically no intermediates are formed. In such cases, the production of hydronium ions directly corresponds to the degradation kinetics of the initial compound [35]. This is mainly not the case with more complex molecules, where the change in pH cannot be used for kinetic analysis. However, the pH monitoring during a photocatalytic process gives a valuable insight into the net changes occurring in the investigated system. As can be seen in Fig. 6a/b (curves #6) there is an initial pH drop during the first 1 hour of irradiation, possibly due to the formation of acidic intermediates. The pH value decreased down to 4 in the case of TiO_2 Wackherr and to 5 in the case of Degussa P25. Interestingly, the pH increase after the 1-hour minimum has a parallel trend to the time evolution of ammonium. This is consistent with previous findings that the release of NH_4^+ under photocatalytic conditions consumes H^+ [36].

Based on the TOC measurements it was concluded that after MET complete removal, about 33% of organic compounds (measured as organic carbon) still remained in the system with Degussa P25, and 89% with TiO_2 Wackherr. After 240 min of irradiation, the percentage of remaining organic compounds decreased to 4% for Degussa P25 and 17% for TiO_2 Wackherr.

Based on all the above, it can be concluded that TiO_2 Wackherr is more efficient as catalyst in the degradation of the starting compound, whereas the complete mineralization is faster in the presence of Degussa P25. Note that substrate degradation and complete mineralization are rather different phenomena that are influenced by different photocatalyst features. The initial degradation rate of a substrate is driven by the reactivity between the substrate itself and the active sites present on the catalyst surface and, obviously, by the number of these sites. The resulting degradation rate could be decreased to a variable extent by the back reactions, which lead to the recombination of the partially oxidized radicals with conduction-band electrons [23,30]. The less important role of the back reactions would largely account for the faster MET disappearance with TiO_2 Wackherr. In contrast,

mineralization is a target that requires quite a long time to be reached and that can be influenced by additional processes, which could not be operational in the early stages of the reaction. One of these processes could be the poisoning of the catalyst surface upon adsorption of certain reaction intermediates/products, which could inhibit further degradation reactions [37]. Poisoning is expectedly more problematic for photocatalysts with lower surface area (such as TiO_2 Wackherr), which have a lower number of active sites that could more easily be blocked. A reasonable consequence could thus be the slower MET mineralization with TiO_2 Wackherr compared to Degussa P25.

3.6. Intermediates and mechanism of photodegradation

The degradation of organic pollutants is often accompanied by the formation of intermediates that can potentially be harmful to the environment [38,39]. To detect and identify potential intermediates, use was made of the LC–DAD and LC–MS/MS techniques. On the basis of the chromatograms shown in Figs. 2a/b and 7 it can be concluded that a number of compounds were formed. The identified intermediates (Fig. 7, Table 1) and the kinetic results (Fig. 8) allowed for the proposal of a possible mechanism for MET photocatalytic degradation (Fig. 9).

Fig. 7 gives the LC–MS chromatograms of MET and its intermediates registered after 240 min of photocatalytic degradation in the presence of Degussa P25 and/or TiO_2 Wackherr (some of the detected intermediates were specific of a particular photocatalyst). Fig. 8 shows the kinetics of formation/disappearance of the intermediates upon irradiation. The figure shows that intermediates **2**, **5**, **8**, **9** and **10** were formed in larger amount in the case of Degussa P25, whereas compounds **3**, **7**, **11**, **12** and **13** were more concentrated in the presence of TiO_2 Wackherr. Compound **4** was present at approximately equal concentration in both cases. Compound **6** was peculiarly identified only with TiO_2 Wackherr and only after 240 min irradiation. In contrast, compounds **14** and **15** were only detected with Degussa P25.

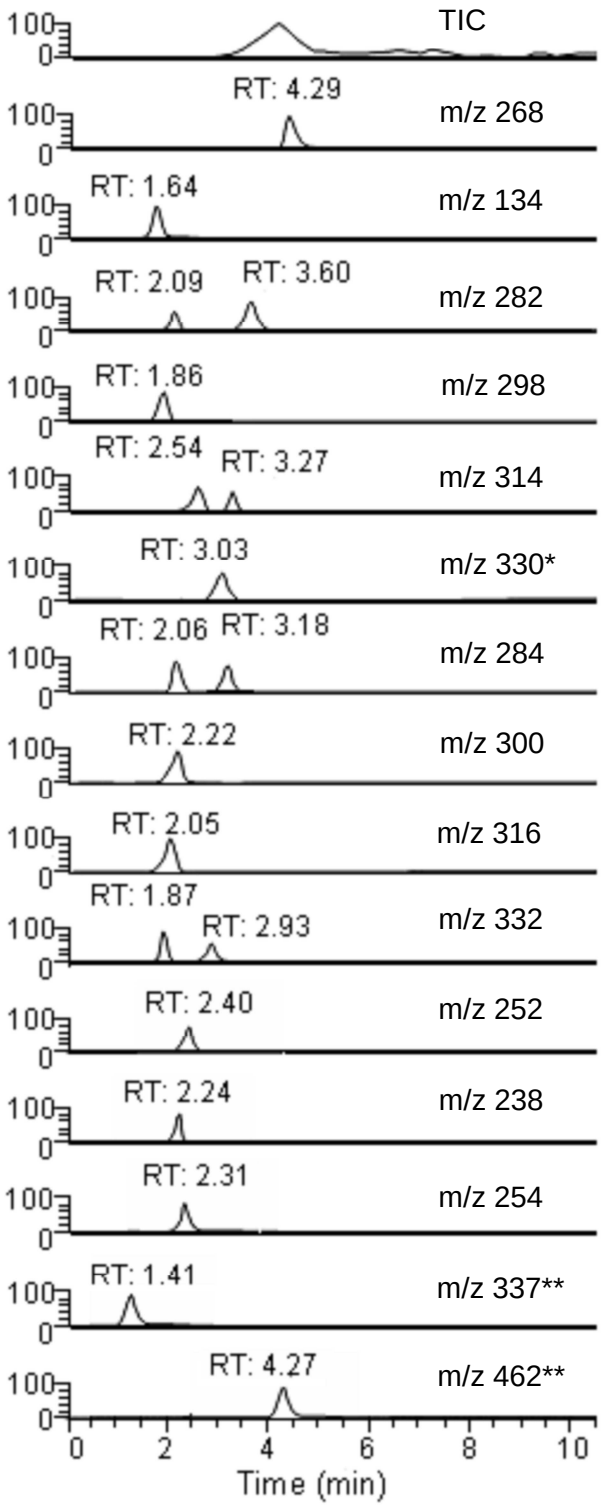

Fig. 7. LC–MS total ion chromatogram (TIC) and extracted ions chromatograms of MET and its intermediates, obtained after 240 min of photocatalytic degradation of MET (3 mM).
* only found with TiO_2 Wackherr, ** only found with TiO_2 Degussa P25.

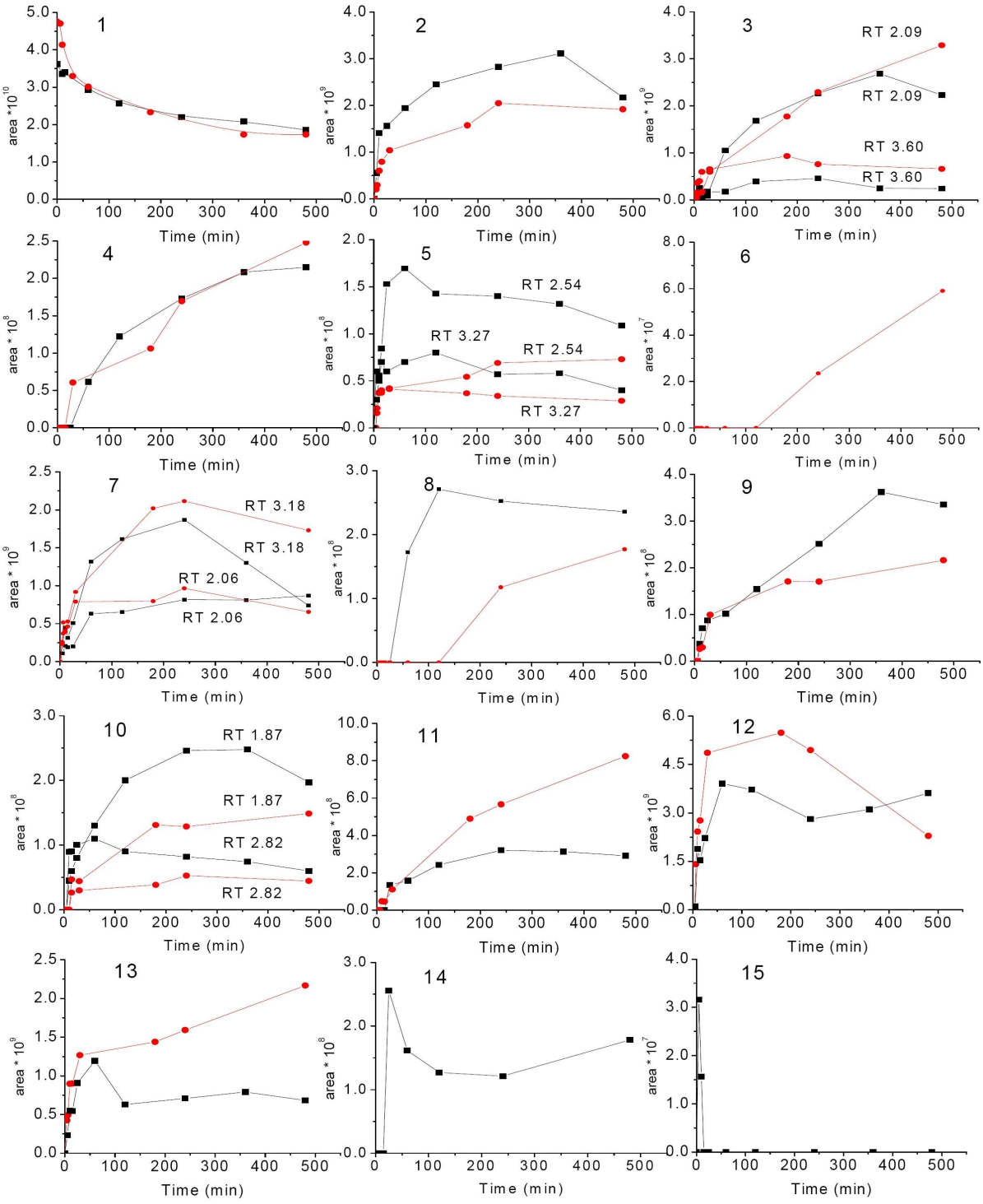

Fig. 8. Kinetics of the photocatalytic degradation of MET (**1**) and of the appearance/disappearance of the intermediates (**2–15**), detected by LC–MS/MS (ESI+). ● TiO_2 Wackherr, ■ Degussa P25.

The different kinetics and the detection of some different intermediates with the two photocatalysts suggest that the degradation pathways with TiO_2 Wackherr and Degussa P25 might not be identical. On the basis of the identified intermediates and of the kinetic data, we propose a tentative scheme of MET photocatalytic degradation (Fig. 9).

In a first stage, after the breaking of a C-C bond in the aliphatic part of the MET molecule (**1**), amino-diol **2** was identified as one of the dominant intermediates. Intermediate **2** was also identified by Yang et al. and Romero et al. [19,20]. The attack of $^{\bullet}OH$ on the C atom next to the ether oxygen and the oxidation of the hydroxyl group would yield the keto-tautomer **3**, which forms two peaks at retention times 2.09 and 3.60 min (Fig. 7)**.** Such a reaction mechanism via keto-enol tautomers has been previously reported for the photo-Fenton degradation of diclofenac [5]. In the case of TiO_2 photocatalytic degradation the enol tautomer was more abundant than the keto derivative, whereas in photo-Fenton experiments they have been detected in comparable amount [40].

The attack of the $^{\bullet}OH$ on the C atoms of the aromatic ring of compound **3** yielded the hydroxy (**4**) and dihydroxy (**5**) intermediates in the presence of both catalysts, and the trihydroxy intermediate (**6**) only in the case of TiO_2 Wackherr. Similarly, the binding of $^{\bullet}OH$ to the benzene ring of the MET molecule resulted in the mono- (**7)**, di- (**8**), tri- (**9**) and tetrahydroxy (**10**) intermediates. Based on the LC–MS/MS chromatograms (Fig. 7), it can be seen that the peaks of intermediate **7** appear at two retention times, *viz.* 2.06 and 3.18 min, probably as a consequence of the possibility to bind a hydroxyl group in the positions of the benzene ring in *meta* or *para* with respect to the methoxyethyl group. Intermediates **7–10** were also identified by Yang et al. [19]. On the other hand, Romero et al. identified an intermediate with m/z (+) 300 which would correspond to our intermediate **8**, but they proposed a different structure that involved the opening of the aromatic ring [20].

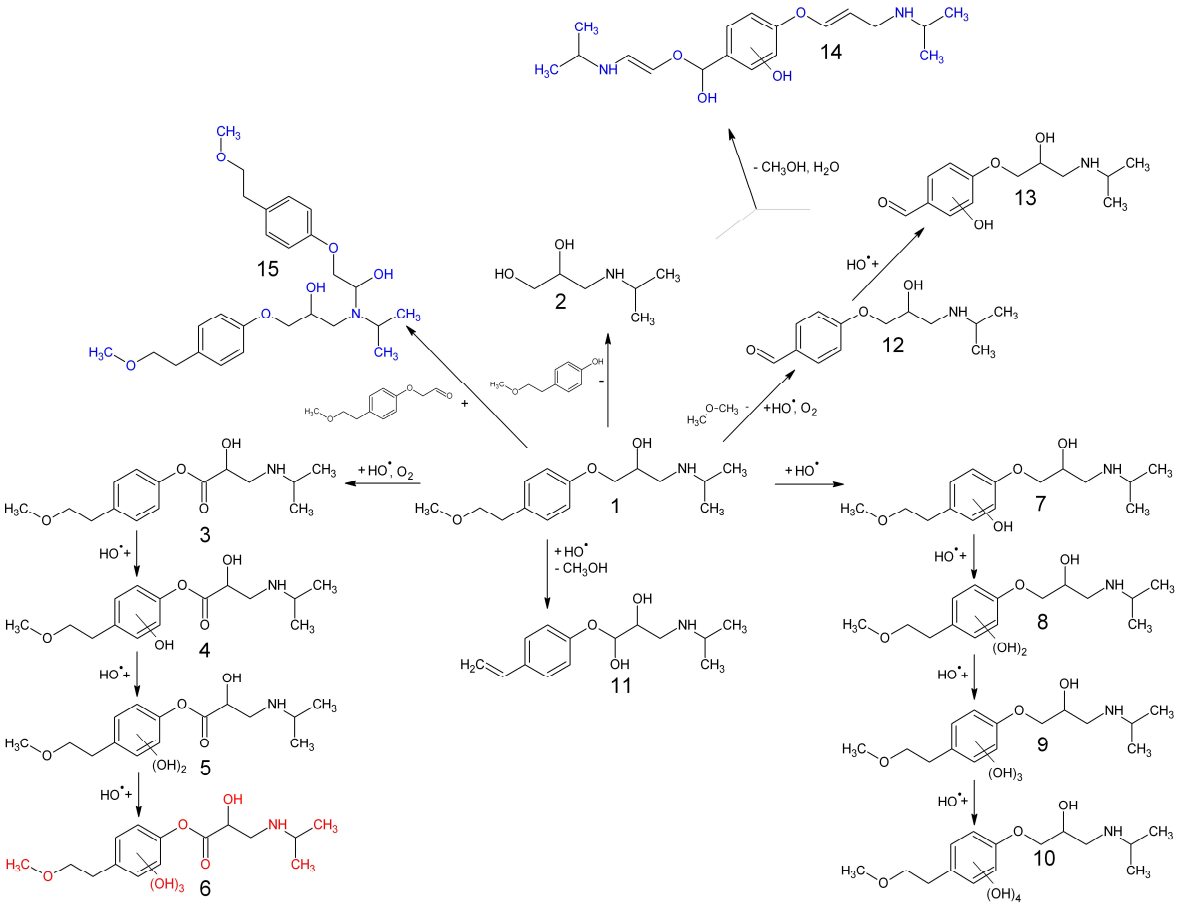

Fig. 9. Tentative pathways for the photocatalytic degradation of MET. Note that **6** was only identified with TiO_2 Wackherr, **14** and **15** only with Degussa P25.

The intermediate **11** could be formed by loss of methanol combined with attack of •OH on the C atom next to the ether oxygen in the aliphatic part of the MET.

The intermediate **12** could be formed by loss of the ether group, abstraction of hydrogen possibly upon •OH radical attack on the alkyl group, and addition of an oxygen atom. Attack of •OH on the C atom of the aromatic ring of **12** could yield the hydroxylated intermediate **13**. The aromatic ring of **12** has two possible positions where the hydroxyl attack could take place, thus one might expect to find two chromatographic **13** peaks as in the case of **7**. The fact that only one peak was found for **13** is probably the consequence of the fact that the –CHO substituent on the **12** aromatic ring has an electron-withdrawing and *meta*-orientating character, while the other substituent is an alkoxy group with an electron-donating and *ortho*/*para* orientating character [40]. Therefore, the effects of both substituents would favor the •OH attack on the position in *meta* to the –CHO group.

During the degradation in the suspension of Degussa P25, it is likely that compound **2** reacts with intermediate **13** and, upon release of methanol and water, produces intermediate **14**. Another intermediate identified with Degussa P25 alone is the dimeric species **15**, in agreement with the work of Kumar et al. [41]. However, this intermediate appeared only at the beginning of the degradation, when the MET concentration was high.

Compounds **14** and **15** were identified in the presence of Degussa P25 but not with TiO_2 Wackherr. The effect of ethanol addition suggests that the reaction with h^+ was more important for TiO_2 Degussa P25 compared to Wackherr, and it is thus possible that the formation of **14** and **15** involves reaction with h^+. Reaction with $^\bullet OH$ is expected to be slightly more important for TiO_2 Wackherr than for Degussa P25. Coherently, the intermediate observed with TiO_2 Wackherr only (**6**) is a polyhydroxylated compound that would likely be produced by $^\bullet OH$ reaction.

All the intermediates underwent final degradation to CO_2, H_2O, NH_4^+ and NO_3^-. The formation of CO_2 and H_2O was postulated on the basis of TOC measurements (Fig. 6a/b, curves #3), and the complete mineralization was attained after over 4 h irradiation.

4. Conclusions

The efficiency of the photocatalytic degradation of MET, a widely used β_1-blocker, was studied in TiO_2 suspensions of Degussa P25 and Wackherr. The photocatalytic degradation over both photocatalysts was considerably more efficient than the direct UV photolysis, and the transformation of the substrate was significantly faster in the presence of TiO_2 Wackherr compared to Degussa P25. The photocatalytic degradation with TiO_2 Wackherr was more efficient especially at high substrate concentration, because this photocatalyst is less affected by the decrease of the degradation rate at elevated substrate concentration (back reactions). This issue can largely compensate for the much lower surface area of TiO_2 Wackherr compared to Degussa P25 (8.5 *vs.* 50 $m^2\ g^{-1}$).

The MET photodegradation by TiO_2 Wackherr generated UV-absorbing intermediates at a relatively higher concentration than Degussa P25. Mineralization of MET was achieved in both cases after about 4 h irradiation, but it faster in the case of Degussa P25 despite the slower initial degradation rate of the substrate. The MET nitrogen atoms were converted predominantly into NH_4^+ and to a lesser extent into NO_3^-. The inhibition of photocatalytic

degradation observed in the presence of ethanol as a hydroxyl radical scavenger suggests that the process mainly involves $^{\bullet}OH$, especially in the case of TiO_2 Wackherr.

The mechanism of photocatalytic degradation was investigated in detail. Fourteen intermediates were identified by LC–MS/MS (ESI+). Hydroxylation of the aromatic ring, shortening of the methoxyl-containing lateral chain and cleavage of, or addition of $^{\bullet}OH$ to, the amine-containing one are the main pathways involved into the photocatalytic degradation process. In the case of Degussa P25, species arising from dimerization or combination of intermediates were also identified.

Acknowledgments

This document has been produced with the financial assistance of the European Union (Project HU-SRB/0901/121/116 OCEEFPTRWR Optimization of Cost Effective and Environmentally Friendly Procedures for Treatment of Regional Water Resources). The contents of this document are the sole responsibility of the University of Novi Sad Faculty of Sciences and can under no circumstances be regarded as reflecting the position of the European Union and/or the Managing Authority. The authors greatly appreciate the financial support from the Ministry of Education and Science of the Republic of Serbia (project no. 172007).

References

[1] C.G. Daughton, T.A. Ternes, Pharmaceuticals and personal care products in the environment: Agents of subtle change?, Environ. Health Persp. 107(suppl.6) (1999) 907–938.

[2] K. Kummerer, Drugs in the environment: Emission of drugs, diagnostic aids and disinfectants into wastewater by hospitals in relation to other sources - a review, Chemosphere 45 (2001) 957–969.

[3] R. Andreozzi, V. Caprio, R. Marotta, A. Radovnikovic, Ozonation and H_2O_2/UV treatment of clofibric acid in water: a kinetic investigation, J. Hazard. Mater.103 (2003) 233–246.

[4] R. Andreozzi, V. Caprio, R. Marotta, D. Vogna, Paracetamol oxidation from aqueous solutions by means of ozonation and H_2O_2/UV system, Water Res.37 (2003) 993–1004.

[5] L.A. Pérez-Estrada, S. Malato, W. Gernjak, A. Agüera, M. Thurman, I. Ferrer, A.R. Fernández-Alba, Photo-Fenton degradation of diclofenac: identification of main intermediates and degradation pathway, Environ. Sci. Technol. 39 (2005) 8300–8306.

[6] T.A. Ternes, M. Meisenheimer, D. McDowell, F. Sacher, H.-J. Brauch, B. Haist-Gulde, G. Preuss, U. Wilme, N. Zulei-Seibert, Removal of pharmaceuticals during drinking water treatment, Environ. Sci. Technol. 36 (2002) 3855–63.

[7] M.-O. Buffle, J. Schumacher, E. Salhi, M. Jekel, U. von Gunten, Measurement of the initial phase of ozone decomposition in water and wastewater by means of a continuous quench-flow system: application to disinfection and pharmaceutical oxidation, Water Res. 40 (2006) 1884–1894.

[8] B. Halling-Sorensen, S.N. Nielsen, P.F. Lanzky, F. Ingerslev, H.C. Lutzhoft, S.E. Jorgensen, Occurrence, fate and effects of pharmaceutical substances in the environment-a review, Chemosphere 36 (1998) 357–393.

[9] R. Molinari, F. Pirillo, V. Loddo, L. Palmisano, Heterogeneous photocatalytic degradation of pharmaceuticals in water by using polycrystalline TiO_2 and a nanofiltration membrane reactor, Catal. Today 118 (2006) 205–213.

[10] D.W. Kolpin, E.T. Furlong, M.T. Meyer, E.M. Thurman, S.D. Zaugg, L.B. Barber, H.T. Buxton, Pharmaceuticals, hormones, and other organic wastewater contaminants in U.S. streams, 1999-2000: a national reconnaissance, Environ. Sci. Technol. 36 (2002) 1202.

[11] Chatzitakis, C. Berberidou, I. Paspaltsis, G. Kyriakou, T. Sklaviadis, I. Poulios, Photocatalytic degradation and drug activity reduction of chloramphenicol, Water Res. 42 (2008) 386–394.

[12] F. Mendez-Arriaga, S. Esplugas, J. Gimenez, Photocatalytic degradation of non-steroidal anti-inflammatory drugs with TiO_2 and simulated solar irradiation, Water Res. 42 (2008) 585–594.

[13] K. Ikehata, N.J. Naghashkar, M.G. El-Din, Degradation of aqueous pharmaceuticals by ozonation and advanced oxidation processes: a review, Ozone-Sci. Eng. 28 (2006) 353–414.

[14] A.C. Alder, C. Schaffner, M. Majewsky, J. Klasmeier, K. Fenner, Fate of β-blocker human pharmaceuticals in surface water: comparison of measured and simulated concentrations in the Glatt Valley Watershed, Switzerland, Water Res. 44 (2010) 936–948.

[15] F.J. Rivas, O. Gimeno, T. Borralho, M. Carbajo, UV-C radiation based methods for aqueous metoprolol elimination, J. Hazard. Mater.179 (2010) 357–362.

[16] Q.-T. Liu, R.I. Cumming, A.D. Sharpe, Photo-induced environmental depletion processes of β-blockers in river waters, Photochem. Photobiol. Sci. 8 (2009) 768–777.

[17] A. Piram, A. Salvador, C. Verne, B. Herbreteau, R. Faure, Photolysis of β-blockers in environmental waters, Chemosphere 73 (2008) 1265–1271.

[18] O.K. Dalrymple, D.H. Yeh, M.A. Trotz, Review Removing pharmaceuticals and endocrine-disrupting compounds from wastewater by photocatalysis, J. Chem. Technol. Biot. 82 (2007) 121–134.

[19] H. Yang, T. An, G. Li, W. Song, W.J. Cooper, H. Luo, X. Guo, Photocatalytic degradation kinetics and mechanism of environmental pharmaceuticals in aqueous suspension of TiO_2: a case of β-blockers, J. Hazard. Mater. 179 (2010) 834–839.

[20] V. Romero, N. De la Cruz, R.F. Dantas, P. Marco, J. Giménez, S. Esplugas, Photocatalytic treatment of metoprolol and propranolol, Catal. Today 161 (2011) 115–120.

[21] D. Vione, C. Minero, V. Maurino, M.E. Carlotti, T. Picatonotto, E. Pelizzetti, Degradation of phenol and benzoic acid in the presence of a TiO_2-based heterogeneous photocatalyst, Appl. Catal. B: Environ. 58 (2005) 79–88.

[22] N. Mahmoodi, M. Arami, N.Y. Limaee, N.S. Tabrizi, Decolorization and aromatic ring degradation kinetics of direct red 80 by UV oxidation in the presence of hydrogen peroxide utilizing TiO_2 as a photocatalyst, Chem. Eng. J. 112 (2005) 191–196.

[23] C. Minero, D. Vione, A quantitative evalution of the photocatalytic performance of TiO_2 slurries, Appl. Catal. B: Environ. 67 (2006) 257−269.

[24] B. Abramović, D. Sojić, V. Despotović, D. Vione, M. Pazzi, J. Csanádi, A comparative study of the activity of TiO_2 Wackherr and Degussa P25 in the photocatalytic degradation of picloram, Appl. Catal. B: Environ. 105 (2011) 191–198.

[25] D. Vione, V. Maurino, C. Minero, M. Vincenti, E. Pelizzetti, Formation of nitrophenols upon UV irradiation of phenol and nitrate in aqueous solutions and in TiO_2 aqueous suspensions, Chemosphere 44 (2001) 237−248.

[26] S. Parra, J. Olivero, C. Pulgarin, Relationships between physicochemical properties and photoreactivity of four biorecalcitrant phenylurea herbicides in aqueous TiO_2 suspension, Appl. Catal. B: Environ. 36 (2002) 75–85.

[27] M. Atiqur Rahman, M. Muneer, Heterogeneous photocatalytic degradation of picloram, dicamba, and floumeturon in aqueous suspensions of titanium dioxide, J. Environ. Sci. Health 40 (2005) 247–267.

[28] M. Qamar, M. Muneer, D. Bahnemann, Heterogeneous photocatalysed degradation of two selected pesticide derivatives, triclopyr and daminozid in aqueous suspensions of titanium dioxide, J. Environ. Manage. 80 (2006) 99–106.

[29] C. Minero, Kinetic analysis of photoinduced reactions at the water semiconductor interface, Catal. Today 54 (1999) 205–216.

[30] C.C. Wong, W. Chu, The direct photolysis and photocatalytic degradation of alachlor at different TiO_2 and UV sources, Chemosphere 50 (2003) 981–987.

[31] S. Mozia, M. Tomaszewska, A.W. Morawski, Photocatalytic degradation of azo-dye acid red 18, Desalination 185 (2005) 449−456.

[32] M.E. Carlotti, E. Ugazio, L. Gastaldi, S. Sapino, D. Vione, I. Fenoglio, B. Fubini, Specific effects of single antioxidants in the lipid peroxidation caused by nano-titania used in sunscreen lotions, J. Photochem. Photobiol. B: Biol. 96 (2009) 130−135.

[33] N. Daneshvar, D. Salari, A.R. Khataee, Photocatalytic degradation of azo dye acid red 14 in water on ZnO as an alternative catalyst to TiO_2, J. Photochem. Photobiol. A: Chem. 162 (2004) 317–322.

[33a] J.F. Montoya, J.A. Velasquez, P. Salvador, The direct–indirect kinetic model in photocatalysis: A reanalysis of phenol and formic acid degradation rate dependence on photon flow and concentration in TiO_2 aqueous dispersions, Appl. Catal. B: Environ. 88 (2009) 50–58.

[34] B.F. Abramović, V.B. Anderluh, A.S. Topalov, F.F. Gaál, Titanium dioxide mediated photocatalytic degradation of 3-amino-2-chloropyridine, Appl. Catal. B: Environ. 48 (2004) 213–221.

[35] J. Theurich, M. Lindner, D.W. Bahnemann, Photocatalytic degradation of 4-chlorophenol in aerated aqueous titanium dioxide suspensions: a kinetic and mechanistic study, Langmuir 12 (1996) 6368–6376.

[36] A. Topalov, B. Abramović, D. Molnár-Gábor, J. Csanádi, O. Arcson, Photocatalytic oxidation of the herbicide (4-chloro-2-methylphenoxy)acetic acid (MCPA) over TiO_2, J. Photochem. Photobiol. A: Chem. 140 (2001) 249−253.

[37] I. Salem, N. Keller, V. Keller, Photocatalytic removal of monoterpenes in the gas phase. Activity and regeneration, Green Chem. 11 (2009) 966–973.

[38] X. Cai, J. Ye, G. Sheng, W. Liu, Time-dependent degradation and toxicity of diclofop-methyl in algal suspensions, Environ. Sci. Pollut. Res. 4 (2009) 459−465.

[39] S. Chiron, L. Comoretto, E. Rinaldi, V. Maurino, C. Minero, D. Vione, Pesticide by-products in the Rhône delta (Southern France). The case of 4-chloro-2-methylphenol and of its nitroderivative, Chemosphere 74 (2009) 599−604.

[40] M. Huber, S. Canonica, G.-Y. Park, U. von Gunten, Oxidation of pharmaceuticals during ozonation and advanced oxidation processes, Environ. Sci. Technol. 37 (2003), 1016–1024.

[41] V. Kumar, R.P. Shah, S. Malik, S. Singh, Compatibility of atenolol with excipients: LC–MS/TOF characterization of degradation/interaction products, and mechanisms of their formation, J. Pharmaceut. Biomed. 49 (2009) 880–888.

Table 1. Intermediates proposed structures for the photocatalytic degradation of MET

Compound	**Precursor ion $[M+H]^+$**	**Molecular formula**	**Name of compound**	**Collision energy (%)**	**MS^2 product ion** (*m/z*, % rel. abundance)	**Collision energy for MS^2 product ion**	**MS^3 product ion[§]** (*m/z*, % rel. abundance)
1	268	$C_{15}H_{25}NO_3$	1-[4-(2 methoxyethyl)phenoxy]-3-(propan-2-ylamino)propan-2-ol	35	116(51), 159(25), 176(26), **191(100)**, 218(66), 226(29), 250(26)	30	159(100)
2	134	$C_6H_{15}NO_2$	3-(propan-2-ylamino)propane-1,2-diol	30	74(21), 92(64), **116(100)**	28	72(100)
3	282	$C_{15}H_{23}NO_4$	4-(2-methoxyethyl)phenyl 2-hydroxy-3-(propan-2-ylamino)propanoate	33	116(23), **159(100)**, 176(24), 205(48), 240(59), 264(34)	33	131(100), 141(31)
4	298	$C_{15}H_{23}NO_5$	Hydroxy derivative 4-(2-methoxyethyl)phenyl 2-hydroxy-3-(propan-2-ylamino)propanoate	33	116(42), 175(21), 252(38) 256(33), 266(51), **280(100)**	32	120(22), 147(24), 175(91), 176(65), 192(100), 221(23), 252(22)
5	314	$C_{15}H_{23}NO_6$	Dihydroxy derivative 4-(2-methoxyethyl)phenyl 2-hydroxy-3-(propan-2-ylamino)propanoate	32	264(20), **282(100)**, 286(35) 296(99)	33	176(25), 210(62), 236(44), 238(75), 252(100), 264(38)
6*	330	$C_{15}H_{23}NO_7$	Trihydroxy derivate 4-(2-methoxyethyl)phenyl 3-[(1-methylethyl)amino]propanoate	32	134(45), 215(21), 284(27), 286(40), 298(29), 302(56), **312(100)**, 330(34)		
7	284	$C_{15}H_{25}NO_4$	Hydroxy derivative 1-[4-(2 methoxyethyl) phenoxy]-3-(propan-2-ylamino)propan-2-ol	33	116(94), 175(48), 191(43), 207(52), 234(39), 242(19), **266(100)**	31	191(23), 192 (36), 207 (23), 234 (100)
8	300	$C_{15}H_{25}NO_5$	Dihydroxy derivative 1-[4-(2 methoxyethyl) phenoxy]-3-(propan-2-ylamino)propan-2-ol	35	250(26), 258(84), 268(55), **282(100)**, 300(22)	33	240(28), 250(100), 264(20)
9	316	$C_{15}H_{25}NO_6$	Trihydroxy derivate 1-[4-(2 methoxyethyl) phenoxy]-3-(propan-2-ylamino)propan-2-ol	33	116(27), 274(85), **298(100)**	30	98(100), 256(23), 266(55), 280(69), 298(28)
10	332	$C_{15}H_{25}NO_7$	Tetrahydroxy derivate 1-[4-(2 methoxyethyl) phenoxy]-3-(propan-2-ylamino)propan-2-ol	30	282(46), 300(44), **314(100)**	28	282(100), 296(47)

11	252	$C_{14}H_{21}NO_3$	1-(4-ethenylphenoxy)-3-(propan-2-ylamino)propane-1,2-diol	33	133(24), **175(100)**, 210(59), 220(21), 234(32)	28	147(100)
12	238	$C_{13}H_{19}NO_3$	4-[2-hydroxy-3-(propan-2 ylamino)propoxy]benzaldehyde	33	161(64), **196(100)**, 220 (32)	28	74(34), 161(100), 178(49)
13	254	$C_{13}H_{19}NO_4$	Hydroxy derivative 4-[2-hydroxy-3-(propan-2-ylamino)propoxy]benzaldehyde	34	116(22), **177(100)**, 212(45), 236(22)	34	159(100)
14**	337	$C_{18}H_{28}N_2O_4$	Hydroxy derivative (4-{[(1*E*)-3-(propan-2-ylamino)prop-1-en-1-yl]oxy}phenyl){[(*E*)-2-(propan-2-ylamino)ethenyl]oxy}methanol	35	260(24), 278(20), 295(45), 300(20), **319(100)**	29	234(86), 259(62), 291(22), 301(100), 319(22)
15**	462	$C_{26}H_{39}NO_6$	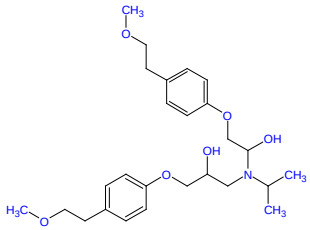	30	388(24), 430(70), **444(100)**, 461(23)	30	270(46), 308(31), 322(30), 360(44), 382(33), 398 (44), 412(100), 426(62)

* intermediates in case of TiO_2 Wackherr, ** intermediates in case of Degussa P25

§ - Precursor ion is marked with bold.